Shape Factors and Cross-Sectional Risk

A New Measure and its Empirical Implications for Portfolio Risk Management

Stefano Galluccio
BNP Paribas London

Andrea Roncoroni*
ESSEC Business School

*Andrea Roncoroni (*corresponding author*): Finance Department, ESSEC Business School, Avenue Bernard Hirsch BP 105, 95021 Cergy-Pontoise, France. Tel.: +33134433239; Fax.: +33134433212; E-mail: andrea.roncoroni@gmail.com; Stefano Galluccio, Fixed Income Derivatives Research, BNP Paribas, 10 Harewood Avenue, NW1 6AA, London, United Kingdom. Tel.: +442075953991; Fax.: +442075955052, E-mail: stefano.galluccio@bnpparibas.com.

Key words: Risk Measures, Risk Management, Factor Analysis, Cross-Sections, Interest Rates.
JEL Classification numbers: C31, E43, G11.

Shape Factors and Cross-Sectional Risk

A New Measure and its Empirical Implications for Portfolio Risk Management

Abstract

Litterman, Scheinkman, and Weiss (1991) and Engle and Ng (1993) provide empirical evidence of a relation between yield curve shape and volatility. This study offers theoretical support for that finding in the general context of cross-sectional time series. We introduce a new risk measure quantifying the link between cross-sectional shape and market risk. A simple econometric procedure allows us to represent the risk experienced by cross-sections over a time period in terms of independent factors reproducing possible cross-sectional deformations. We compare our risk measure to the traditional cross-yield covariance according to their relative performance. Empirical investigation in the US interest rate market shows that 1) cross-shape risk factors outperform cross-yield risk factors (*i.e.*, yield curve level, slope, and convexity) in explaining the market risk of yield curve dynamics; 2) hedging multiple liabilities against cross-shape risk delivers superior trading strategies compared to those stemming from cross-yield risk management.

1 Introduction and Summary of Results

Financial risk management aims at reducing the unpredictable effect of volatile market conditions on the value of investment portfolios. Traditionally, this variability is evaluated through dispersion measures of the portfolio value around its expected average return. Assessing these figures requires some hypotheses about the random evolution of factors determining the value of all positions in the portfolio.[1] Beyond the problem of data availability, modeling market determinants is a challenging task due to their heterogeneity and high number.

One way to reduce factor heterogeneity is to identify and sort basic financial quantities (*e.g.*, yields, asset prices, implied volatilities) along one or more cross-sectional dimensions.[2]Modeling cross-sectional dynamics is a difficult task due the high number of involved variables. In principle, there is one variable per observation along each cross-sectional dimension. The issue of identifying and hedging against a reduced number of significant factors has been extensively dealt with in the context of interest rate markets. All major traditional approaches to bond portfolio risk management share a common methodology. First, yield curve deformations are selected and linked to a reduced number of underlying factors. Then, the investment portfolio is diversified so as to minimize its sensitivity to yield curve shifts stemming from a perturbation in these factors. However, these approaches differ in the way these shifts are modeled.

One strand of literature assigns specific functional forms to any conceivable yield curve updating. These forms range from parallel shifts as postulated by Redington (1956) and Fisher and Weil (1972) to parametric families of functions as suggested by Chambers, Carleton, and McEnally (1988) and Prisman and Shores (1988), among others. The approach has the remarkable advantage of accounting for full information about the yield curve. Unfortunately, it provides no statistical support for the selected deformations, which are usually chosen on the basis of qualitative considerations. This absence may hinder the effectiveness of hedging strategies grounded on this approach.

Another branch of literature identifies factors in a few benchmark yields (*e.g.*, Elton, Gruber, and Michaely (1990)), or particular linear combinations of them, usually

determined by means of statistical analysis (*e.g.*, Litterman and Scheinkman (1991)). In the latter case, factors are ranked according to their contribution to the historical market volatility and the first few significant ones are retained for the purpose of representing market risk. This approach dramatically simplifies the selection of effective risk management strategies. However, and in contrast with the aforementioned functional approach, the method is irrespective of the typical shapes displayed by time series of yield curves and leave the corresponding information unaccounted for.[3]In particular, it ignores any possible link between *cross-sectional shape* and *market volatility.*

In the context of interest rate markets, Litterman, Scheinkman, and Weiss (1991) report evidence of strong correlation between interest rate volatility and yield spreads of certain butterfly positions representing yield curve shape through its convexity; Engle and Ng (1993) show that empirical yield curve deformations can be explained by combining expected short-term rate changes and term premia, which in turn are related to a volatility factor through the standard APT.

Motivated by these findings, we introduce a new measure of risk accounting for the link between cross-sectional shapes and volatility and provide an empirical assessment of its performance in the U.S. Treasury Bond market. Our presentation is organized along three logical steps. First, we record the empirical covariance experienced by cross-sectional shapes on a given time period. This is our measure of cross-sectional risk and we refer to it as cross-shape risk. Next, we decompose this risk into analytic cross-sectional deformations representing cross-shape risk factors. These steps constitute the main theoretical contribution of the paper. Finally, we compare cross-shape risk to the traditional cross-yield covariance and assess their performance for 1) reproducing the historical market volatility through a reduced number of underlying factors and 2) selecting effective risk management strategies.

We run a backtest simulation and compare two multiperiod bond portfolio strategies, one immunizing against cross-shape risk, the other hedging against cross-yield risk. A first test shows that a limited number of cross-shape factors better accounts for interest rate risk than the same number of cross-yield factors as defined as the

principal components of a cross-yield covariance. Even more interestingly, a second test indicates that the vast majority of trading simulations that immunize against cross-shape risk deliver profit and loss (P&L) distributions displaying a significantly smaller dispersion than those resulting from strategies that hedge against cross-yield risk. These empirical results indicate that our cross-shape risk measure outperforms the cross-yield covariance for the purpose of explaining and managing interest rate volatility.

The paper is organized as follows. Section 2 introduces the notion of cross-shape risk and provides an econometric decomposition of it in terms of ranked cross-sectional deformations. Section 3 highlights the main differences between cross-shape risk and the traditional notion of cross-yield covariance. Section 4 describes the U.S. Treasury bond data used in the empirical analysis. Sections 5 and 6 develop comparative tests on the performance of cross-shape and cross-yield risk measures. Section 7 concludes with a few remarks and suggestions for further research.

2 Cross-Shape Risk

2.1 Model Setting

We consider a financial market where a cross-section $y(t) = \{y(t,\tau), \tau > 0\}$ of interest rates, asset prices, or any other financial index is quoted on each day t. For the purpose of assessing the market risk experienced by the cross-section on a time period, we consider a number N of quoted values $y_1 = y(t,\tau_1), ..., y_N = y(t,\tau_N)$, sorted by time-to-maturity, *i.e.*, $\tau_1 < ... < \tau_N$. Absolute returns $\Delta y_i := y(t+\Delta,\tau_i) - y(t,\tau_i)$ over a period Δ can be linked to factors $z_1, ..., z_N$ representing the systematic (*i.e.*, nondiversifiable) components of market risk through the Linear Return-Generating Gaussian Model adopted by Litterman and Scheinkman (1991):

$$\Delta y_i = \mu_i + \sum_{j=1}^{N} v_i^j z_j + \varepsilon_i. \tag{1}$$

Here the ε_i's represent mutually independent and nonsystematic risk components, each one being idiosyncratic to the corresponding return.[4] This representation suffers

from two shortcomings. First, it does not account for the risk borne by returns not included in the set. This feature undermines the risk analysis of portfolios involving unobservable portions of the cross-section. Moreover, model (1) makes no reference to the shapes exhibited by historical yield curves, which represent important information for the trader.

We propose to modify model (1) and account for a *continuum* of yields by setting

$$\Delta y(\tau) = \mu(\tau) + \sum_{j=1}^{N} v_j(\tau) z_j, \tag{2}$$

where $\mu(\tau)$ denotes the expected shift in the cross-section and $\mathbf{z} = (z_1, ..., z_N) \sim \mathcal{N}_N(\mathbf{0}, I)$ gathers independent and normally distributed sources of market noise. The relationship between cross-sectional shape and risk is accounted for through functions $v_j(\tau)$ $(j = 1, ..., N; \tau \geq 0)$ representing statistically independent curve deformations. Although these latter are usually unobservable, they can be inferred from the market through a simple econometric procedure that generalizes principal components analysis to functional data.

2.2 Model Econometrics

We propose a three-step procedure to define and decompose a measure of cross-sectional risk in terms of statistically independent cross-sectional deformations.

Step I (Cross-sectional fitting). We assume the cross-section is daily recovered as a superposition of a finite number of basis shapes, *i.e.*,

$$y(t, \tau) = \sum_{l=1}^{N} c_l(t) \psi_l(\tau), \tag{3}$$

where each coefficient $c_l(t)$ denotes the curve sensitivity with respect to a small perturbation in the corresponding shape ψ_l at time t. As noted by Anderson *et al.* (1996), these shapes can be selected based on the typical cross-sectional deformations displayed in the market under investigation.

Step II (Cross-sectional risk measurement). The average shift $\mu(\tau)$ in formula (2) and the cross-section of time normalized and centered absolute returns $\Delta\overline{y} := \Delta^{-1/2}[\Delta y - \mu]$

are both linear combinations of basis shapes, *i.e.*,

$$\mu(\tau) = \sum_{l=1}^{N} \mu_l \psi_l(\tau), \text{ and } \Delta\overline{y}(\tau) = \sum_{l=1}^{N} \delta_l \psi_l(\tau), \tag{4}$$

where weighing coefficients are defined by $\mu_l := E[c_l(t+\Delta) - c_l(t)]$ and $\delta_l := \Delta^{-1/2}[c_l(t+\Delta) - c_l(t) - \mu_l]$. The risk borne by yield curve dynamics can be measured through the following dispersion measure of the centered return $\Delta\overline{y}(\tau)$.

Definition 1. The **Cross-Shape Risk** born by a cross-section $y(t,\cdot), t \geq 0$ is the covariance matrix of the vector $\boldsymbol{\delta} = (\delta_1, ..., \delta_N)$ of weighting coefficients, *i.e.*,

$$\mathcal{C}_S(\Delta\overline{y}) := \text{Cov}(\boldsymbol{\delta}). \tag{5}$$

In particular, the **Shape Risk** is the sum of the variances across all coefficients δ_i, *i.e.*, $\mathcal{V}_S(\Delta\overline{y}) := \text{Trace}[\text{Cov}(\boldsymbol{\delta})]$. Naturally, empirical figures over a time period are obtained by replacing the covariance operator with its sample counterpart.

Step III (Factor identification). We assume that the vector gathering yield curve sensitivities to the selected basis shapes is normally distributed with zero mean and covariance matrix Σ, *i.e.*, $\boldsymbol{\delta} = (\delta_1, ..., \delta_N) \sim \mathcal{N}_N(\mathbf{0}, \Sigma)$. If $\Sigma = U\Lambda U^{\mathsf{T}}$ is the corresponding eigenvalue decomposition, with $\Lambda = diag(\lambda_1, ..., \lambda_N)$ $(\lambda_i > \lambda_{i+1})$ and $U = \left[\mathbf{u}^1 \middle| ... \middle| \mathbf{u}^N\right]$ $(\|\mathbf{u}^i\| = 1)$, the set of variables defined by the scalar product

$$z_j := \frac{1}{\sqrt{\lambda_j}} \mathbf{u}^j \cdot \boldsymbol{\delta}, \qquad \text{for } j = 1, ..., N, \tag{6}$$

defines a random vector $\mathbf{z}$ with distribution $\mathcal{N}_N(\mathbf{0}, I)$. By inverting the system of equations (6) with respect to $\boldsymbol{\delta}$, we obtain components $\delta_l = \sum_{j=1}^{N} \sqrt{\lambda_j} u_l^j z_j$, where u_l^j denotes the l-th component of the j-th eigenvector. After plugging these values into expression (4), we finally come up with a linear representation of cross-sectional dynamics in terms of basis shapes and a factor model of the kind (2):

$$\Delta\overline{y}(\tau) = \sum_{l=1}^{N} \left(\sum_{j=1}^{N} \sqrt{\lambda_j} u_l^j z_j \right) \psi_l(\tau) = \sum_{j=1}^{N} v_j(\tau) z_j, \tag{7}$$

with $v_j(\tau) := \sqrt{\lambda_j}\sum_{l=1}^{N} u_l^j \psi_l(\tau)$. Each function v_j represents the effect on the cross-sectional shape caused by a shock in the j-th most significant risk factor z_j. This observation leads to the following

Definition 2. The j-th **Cross-Shape Risk Deformation** driving cross-sectional dynamics (2) is defined as the linear combination of basis shapes $\psi_1, ..., \psi_N$

$$v_j(\tau) := \sum_{l=1}^{N} d_l \psi_l(\tau), \tag{8}$$

with coefficient defined by $d_l = \sqrt{\lambda_j} u_l^j$. According to expression (7), this function can be identified with the j-th **Cross-Shape Risk Factor** z_j driving cross-sectional dynamics.

The key point here is that functions $v_1(\cdot), ..., v_N(\cdot)$ have been selected through a statistically sound method and ranked according to their importance in explaining cross-sectional dynamics. Specifically, each eigenvalue λ_j assesses the quota of shape risk carried by the corresponding factor as measured with respect to a new coordinate system $\left\{ f_j(\tau) := \sum_{l=1}^{N} u_l^j \psi_l(\tau), j = 1, 2, ..., N \right\}$. Consequently, the number of explanatory variables in our model can be reduced by retaining factors whose joint contribution to the shape risk attains a given percentage, and by discarding all the others.

3 Comparison with Cross-Yield Risk

In the context of fixed-income markets, cross-sectional risk is traditionally identified with **Cross-Yield Risk.** This is defined as the sample covariance matrix of a time series of annualized yield increments, usually inferred from market quotations of liquid securities (Steeley (1990), Litterman and Scheinkman (1991), and Hull (2005)). Unfortunately, this measure, and the corresponding factors, do not allow to make any assessment about the risk affecting those portions of the yield curve which are not covered by the set of observed yields, the so-called "non-traded" times-to-maturity. On the contrary, our measure of risk allows to compute the cross-yield covariance over

a *continuum* of times-to-maturity through the simple formula[5]

$$\mathrm{Cov}\left(\Delta y\left(\tau_1\right), \Delta y\left(\tau_2\right)\right) = \sum_{j=1}^{N} v_j\left(\tau_1\right) v_j\left(\tau_2\right). \tag{9}$$

This decomposition shows an explicit link between the magnitude of risk embodied by absolute yield returns and market expectations about the future evolution of the term structure as represented by the cross-shape risk deformations v_j. These latter thus play the double role of 1) typical yield curve shifts and 2) sources of cross-sectional risk.

Recovering risk over the entire time-to-maturity spectrum is particularly important for the computation of price sensitivities of rolling-over hedging portfolios. These strategies usually involve bonds with fixed coupon payment dates. As time goes by, each portfolio adjustment entails computing bond prices and sensitivities for sliding, and then non-traded, times-to-maturity.

If risk is measured by a cross-shape covariance $\mathcal{C}_S$, each coupon sensitivity is given by the corresponding cash flow multiplied by the partial derivative of the corresponding discount bond price with respect to the relevant noise term z_j as defined in formula (6). Recalling the pricing identity $P\left(t,\tau\right) = \exp\left(-y\left(t,\tau\right)\tau\right)$ and adopting the yield curve model $\Delta\overline{y}\left(\tau\right) = \sum_{j=1}^{N} v_j\left(\tau\right) z_j$, the discount bond price sensitivity to the j-th cross-shape factor at time t depends on the cross-shape deformation v_j through

$$\partial_j P\left(t,\tau\right) = -\tau P\left(t,\tau\right) v_j\left(\tau\right),\ \tau \geq 0. \tag{10}$$

If, instead, risk is measured by a cross-yield covariance and dynamics are assigned by $\Delta\overline{y}\left(\tau_i\right) = \sum_{j=1}^{N} \upsilon_i^j z_j$ $(i = 1, ..., N)$, the sensitivity to a factor j can be analytically computed only for zero-coupon bonds corresponding to the selected yields $y\left(\tau_1\right), ..., y\left(\tau_N\right)$ as

$$\partial_j P\left(t,\tau_i\right) = -\tau_i P\left(t,\tau_i\right) \upsilon_i^j, \tag{11}$$

where $\upsilon_i^j := \sqrt{\gamma_j} w_i^j$ are volatility components, coefficients $\gamma_1, \cdots, \gamma_N$ represent the decreasingly ordered eigenvalues of the covariance matrix of centered yield increments $\Delta\overline{y}\left(\tau_1\right), ...,\Delta\overline{y}\left(\tau_N\right)$, and vectors $\mathbf{w}^j = \left(w_1^j, ..., w_N^j\right)^{\mathsf{T}}$ $(j = 1, ..., N)$ denote the corresponding normalized eigenvectors.

In summary, the main quantities involved in cross-yield and cross-shape analyses are:

	Cross-Yield	Cross-Shape
Covariance	$\mathrm{Cov}(\Delta\overline{y}(\tau_1), ..., \Delta\overline{y}(\tau_N))$	$\mathrm{Cov}(\delta_1, ..., \delta_N)$
Eigenvalues	$\gamma_1, \cdots, \gamma_N$	$\lambda_1, \cdots, \lambda_N$
Eigenvectors	$w^1, ..., w^N$	$u^1, ..., u^N$
j-th Deformation	$\upsilon^j := \left(\sqrt{\gamma_j} w_1^j, \cdots, \sqrt{\gamma_j} w_N^j\right)^{\mathrm{T}}$	$v_j(\tau) := \sqrt{\lambda_j} \sum_{l=1}^N u_l^j \psi_l(\tau)$
j-th Sensitivity	$-\tau P(t,\tau)\, \partial_k y(\tau)\, \upsilon_k^j$	$-\tau P(t,\tau)\, v_j(\tau)$

Bond sensitivities at non-traded times-to-maturity must be obtained through interpolation between observed yields. If the fitted yield curve is $y(\tau) = \sum_{l=1}^N b_l \psi_l(\tau)$, then sensitivities read as

$$\partial_j P(t,\tau) = \sum_{k=1}^N \frac{\partial P(t,\tau)}{\partial y(\tau)} \frac{dy(\tau)}{dy(\tau_k)} \upsilon_k^j = -\tau P(t,\tau) \sum_{k=1}^N \left(\sum_{l=1}^N b_l \left[d_\tau \psi_l \right](\tau_k) \right) \upsilon_k^j, \quad (12)$$

where $\left[d_\tau \psi_l \right](\tau_k)$ are ordinary derivatives with respect to time-to-maturity.

Contrary to the cross-shape risk analysis, here interpolation is done *after* performing factor analysis and *the resulting yield sensitivities have no statistical significance*. The key difference of our approach is that yields are first fitted and then the entire yield curve undergoes a principal components analysis based on the history of market dynamics. Consequently, we can obtain a statistically assessed yield volatility function over the whole time-to-maturity spectrum. This is the major theoretical improvement of our methodology compared to the traditional cross-yield risk analysis.

4 Data

In conducting this study, we used data from the U.S. Treasury bond market. The data consist of daily observations for the period from March 1, 1988 to February 28, 2002. Each observation comprises constant maturity par yields referring to the following benchmark times-to-maturity (including selected key rates as reported in RiskMetrics (1996)):[6] 6-month, 1-year, 2-year, 5-year, 7-year, 10-year, 15-year, and

20-year. All data, except the 7-year and the 15-year yields, are obtained from the Bloomberg system. The 7-year and 15-year yields stem from an internal information system at BNP Paribas in London.[7]According to standard market quotation rules, these data include mid-market quotations of Treasury bond yields.

During the examined period, yield curves exhibit four qualitatively distinct shapes: convex, concave, downward humped, and upward humped. Sample curve are displayed in Figure 1.

Insert Figure 1 about here

These forms reflect market anticipations about the future evolution of interest rates. For instance, long-term growth expectations in the economy translate into positively sloped yield curves as demand for long-term investments increases. Symmetrically, gloomy economy forecasts, possibly linked to the economic cycle or sociopolitical events, are reflected in negatively sloped yield curves.

Factors should reproduce the stylized shapes displayed by empirical yield curve fluctuations. This goal can be achieved by selecting a suitable class of basis shapes. We propose to adopt term structure profiles defined by

$$\psi_l(\tau) := \mathcal{L}_l(\tau) \exp(-\zeta\tau), \qquad l = 1, ..., N, \tag{13}$$

where $\mathcal{L}_l(\tau)$ denotes the Laguerre polynomial of order l, and ζ is a positive constant. The first three basis shapes are:

$$\psi_0(\tau) = e^{-\zeta\tau},\ \psi_1(\tau) = e^{-\zeta\tau}(1-\tau),\ \psi_2(\tau) = \frac{e^{-\zeta\tau}}{2}\left(2 - 4\tau + \tau^2\right).$$

This choice is motivated by three heuristic considerations.

First, empirical yield curves in our data set can be recovered by proper linear combinations of these functions (Figure 1) and the same holds for their changes over time. Second, the exponentially decreasing multiplicative factor ensures proper smoothness in the curve outline and adequate interpolation stability under possible shocks affecting single yields.[8]Finally, and more importantly, the chosen set of basis functions spans the range of observed yields quite uniformly. This feature is the direct counterpart of the property requiring evenly lagged yield observations in the traditional

principal components analysis of term structure dynamics. Moreover, as will be shown in the next two sections, it turns out that this is a key property for ensuring a good quality of risk measurement and management performance.

It should be also stressed that our choice is in agreement with several studies proposing alternative functional families to model yield curve dynamics for the purpose of bond portfolio immunization (*e.g.*, Barrett, Gosnell, and Heuson (1995), Navalka and Chambers (1996), Willner (1996), Phoa and Shearer (1997), and Rodrigues De Almeida, Duarte, and Coelho Fernandes (1998), among others).

In summary, our input data consist of a set of discount yields and a number of interpolating basis functions reproducing the qualitative features displayed by empirical yield curves.

5 Risk Measurement

Cross-yield risk has long shaped the way quantitative analysts select driving factors underlying continuous time models of interest rate dynamics, the most important instance being represented by the Heath, Jarrow, and Morton (1992) framework. Moreover, cross-yield factors v^j play an important role in setting trading strategies to hedge against yield curve fluctuations. These considerations suggest taking the cross-yield risk as our benchmark and evaluating the relative performance of cross-shape risk.

A first test compares the speed of risk clustering around uncorrelated factors of the two types.

Insert Table 1 about here

Table 1 shows the percentage quota of the overall empirical risk embodied by the first one, two, three, and four uncorrelated cross-shape and cross-yield factors over four time periods. We see that the first three yield factors capture between 94% and 99% of the total yield risk represented by the sum to all eigenvalues of the cross-yield covariance, whereas the corresponding number embodied in cross-shape factors always reproduce more than 99% of the observed shape risk. We underline that yield

and shape risk numbers need not match, although they refer to a common time-to-maturity.

A second test compares the ability of a reduced number $K < N$ of cross-yield and cross-shape factors to recover the empirical yield risk represented by the sample volatility function across varying times-to-maturity.

The yield volatility function resulting from our cross-shape risk measure obtains by setting $\tau_1 = \tau_2 = \tau$ in formula (9), *i.e.*,

$$\text{Vol}_{\text{cs}}\left(\Delta y\left(\tau\right)\right) := \sqrt{\sum_{j=1}^{K} v_j\left(\tau\right)^2}, \qquad \text{for all } \tau > 0, \tag{14}$$

where shape risk factors are defined in formula (8).

The yield volatility function resulting from a cross-yield risk measure is obtained by interpolating between sample yield risk defined by

$$\text{Vol}_{\text{cy}}\left(\Delta y\left(\tau_i\right)\right) := \sqrt{\sum_{j=1}^{K} \lambda_j {w_i^j}^2}, \qquad \text{for all } \tau_i \ (i = 1, .., N), \tag{15}$$

where w_i^j denotes the i-th component of the eigenvector corresponding to the j-th largest eigenvalue of the cross-yield covariance matrix Γ corresponding to a set of N benchmark times-to-maturity $\tau_1, ..., \tau_N$.[9]

Insert Figure 3 about here

Figure 3 displays yield volatility functions as obtained by selecting the first one, two, three, and four most relevant cross-shape factors (dashed curve) and cross-yield factors (plain line). These are compared to the yield volatility profile experienced by the market over the entire time horizon (dotted path).

Two main considerations arise from an inspection of these graphs. First, cross-shape factors account for yield volatility more accurately than cross-yield factors do in all cases and for most times-to-maturity. For instance, Pérignon and Villa (2006) notice that empirical volatility functions display a hump between the second and the fifth year in the time-to-maturity axis. We see that the volatility function resulting

from cross-shape factors owns this property, whereas the one computed from cross-yield factors does not display this feature. This can be explained by the fact that cross-yield analysis does not account for the unobservable portions of the yield curve, while cross-shape risk analysis makes a precise statistical assessment of all yields recovered by a preliminary interpolation procedure.

The second consideration concerns the speed of convergence of reduced-factor yield volatility functions to the empirical volatility path as the number of factors increases. The volatility function resulting from a cross-shape analysis converges to the sample volatility more rapidly than the one derived by a cross-yield analysis. This effect is in accordance with the quicker convergence of cross–shape eigenvalues than the one displayed by the cross-yield eigenvalues (see Table 1).

The absolute performance of cross-yield and cross-shape risk measures depends on the way input data are built. In the former case, yields should be observed on evenly spaced time-to-maturity lags. A similar property is required for the case of cross-shape risk analysis, where basis functions should span the range of possible yield curves as uniformly as possible. Specifically, if the selected class of functions uncovers some portions of the range spanned by the observed yields over the time-to-maturity spectrum from 0 to 20 years, then interpolation requires relatively large coefficients and a poor risk representation is experienced in those portions of the yield curve. We support this conjecture by a further empirical test comparing cross-shape analyses conducted on a common data set under alternative bases. We consider exponentially weighted Laguerre, Legendre and Chebyshev polynomials, as reported in Appendix A. In all cases, functional uniformity is followed by a good reproduction of the empirical volatility function. Figure 4 shows this effect in the case of Laguerre and Chebyshev polynomials.

Insert Figure 4 about here

In summary, cross-sectional risk proves to be a more efficient and effective measure of market variability than the traditional notion of cross-yield risk. This observation paves the way to cross-shape risk management as a viable alternative to the classical factorial hedging strategies based on cross-yield risk factors. We empirically

investigate this conjecture in the following section.

6 Risk Management

We perform a back-test analysis to assess the relative ability of cross-shape and cross-yield risk measures to properly drive portfolio selection for risk management purposes in a fixed income market. Specifically, we consider bond portfolios immunizing a multiple liability against the interest rate risk experienced in the US Treasury bond market during the last decade. Empirical market risk is alternatively measured by the cross-shape and the cross-yield covariance. This leads to a pair of trading strategies, the former hedging against cross-shape risk, the latter neutralizing cross-yield risk. We refer to these as the "cross-shape strategy" and the "cross-yield strategy", respectively. Barber and Copper (1996), Willner (1996), and Soto (2004), among others, document the superiority of the cross-yield strategy over trading driven by alternative risk measures. Accordingly, we select this methodology as a benchmark to compare the performance of our cross-shape strategy. The analysis is based on distributional properties of the two P&L streams generated by the net portfolio consisting of the hedging asset positions minus the selected outstanding liability.

6.1 Test Design

We formulate our risk management test in terms of a multiperiod immunization program as seen from current date 0. An outstanding liability is given as a multiple cash flow maturing at a future time T. Our goal is to hedge this position value against the effects caused by interest rate fluctuations occurring during the contract lifetime.

We perform hedging by trading in the bond market. Tradeable bonds are indexed by $\alpha = 1, ..., m$, and the issued liability is labelled $\alpha = 0$. We assume that each bond α is issued *at par* upon inception, *i.e.*, the initial price equals face value N^α and α pays out n^α constant coupons with annual frequency, beginning exactly one year after the strategy outset. The *par* condition determines a unique constant coupon as

$$c^\alpha = \frac{N^\alpha \left(1 - P\left(0, n^\alpha\right)\right)}{\sum_{i=1}^{n^\alpha} P\left(0, i\right)}, \qquad \alpha = 0, 1, ..., m.$$

We suppose the trading horizon $[0,T]$ splits into exactly n periods with uniform length Δ (years), *i.e.*, $n\Delta = T$, and we form a dynamic portfolio of tradeable bonds in a way that the joint position with the outstanding liability is as immune as possible to the effects of yield curve fluctuations on each trading date $k\Delta$, $k = 1, ..., n$. This goal can be achieved by a three-step procedure.

Step 1 (P&L recording). We register a possible gap between the bond portfolio price and the present value of the outstanding liability as occurred on the period elapsed since the last trading day. This mismatch contributes to the trader's P&L. If $\mathbf{B}(k) = (B_1(k), ..., B_m(k))^{\mathsf{T}}$ gathers all tradeable coupon-bond prices at time $k\Delta$ and $L(k)$ indicates the time $k\Delta$ value of the outstanding liability, the realized P&L streams from the two strategies over the period $\Delta_k = [(k-1)\Delta, k\Delta]$ read as

$$\text{P\&L}_{\text{cs}}(k) = \mathbf{B}(k) \cdot \mathbf{q}(k-1) - L(k) , \tag{16}$$

$$\text{P\&L}_{\text{cy}}(k) = \mathbf{B}(k) \cdot \boldsymbol{\chi}(k-1) - L(k) , \tag{17}$$

where $\mathbf{q}(k) = (q_1(k), ..., q_m(k))^{\mathsf{T}}$ (resp. $\boldsymbol{\chi}(k) = (\chi_1(k), ..., \chi_m(k))^{\mathsf{T}}$) denotes the vector of bond positions held between consecutive trading dates $k\Delta$ and $(k+1)\Delta$ under the cross-shape (resp. cross-yield) strategy.

Step 2 (Risk updating). We update the outstanding risk measurement and the resulting risk factors. Cross-shape factors issue from the cross-shape risk measure, while cross-yield factors result from the cross-yield risk measure as computed on a time series including historical yield curves observed in the last period.

Step 3 (Dynamic hedging). We change our bond selection in a way that the resulting portfolio is: a) self-financing, and b) as sensitive to the updated risk factors as to the outstanding liability. Self-financing means that no wealth is created nor required for adjusting the portfolio composition. In other words, the rebalanced portfolio must be exclusively funded by the proceeds resulting from liquidating the standing portfolio plus any increase in the liability value since the last trading day. This imposes the first constraint on the bond portfolio mix $\mathbf{q}(k)$ (resp. $\boldsymbol{\chi}(k)$), that is

$$\mathbf{B}(k) \cdot \mathbf{q}(k) = \mathbf{B}(k) \cdot \mathbf{q}(k-1) + L(k) - L(k-1) , \tag{18}$$

$$\mathbf{B}(k) \cdot \boldsymbol{\chi}(k) = \mathbf{B}(k) \cdot \boldsymbol{\chi}(k-1) + L(k) - L(k-1) . \tag{19}$$

The condition is initialized by supposing that all proceeds from the liability issue are immediately reinvested in the hedging portfolio, namely

$$\begin{aligned} \mathbf{B}(0) \cdot \mathbf{q}(0) &= L(0), \\ \mathbf{B}(0) \cdot \boldsymbol{\chi}(0) &= L(0). \end{aligned} \tag{20}$$

These formulae are clarified in Appendix B.

Additional d constraints stem from neutralizing the net portfolio value against market moves driven by the same number of selected principal factors. A bond portfolio (or liability) sensitivity to a given factor reduces to a linear combination of discount bond sensitivities, which we compute through formulae (10) and (12). The resulting constraints are obtained by matching asset and liability sensitivities.

The cross-shape strategy satisfies the first-order constraints

$$\nabla \mathbf{B}_{\text{cs}}(k) \cdot \mathbf{q}(k) = \nabla L_{\text{cs}}(k), \tag{21}$$

where the (j,i)-entry of matrix $\nabla \mathbf{B}_{\text{cs}}(k)$ contains the sensitivity of the i-th hedging bond to the j-th cross-shape factor prevailing at time $k\Delta$, and vector $\nabla L_{\text{cs}}(k)$ gathers all liability sensitivities to the same factors.

Similarly, the cross-yield strategy satisfies the first-order conditions

$$\nabla \mathbf{B}_{\text{cy}}(k) \cdot \boldsymbol{\chi}(k) = \nabla L_{\text{cy}}(k), \tag{22}$$

where the (j,i)-entry of matrix $\nabla \mathbf{B}_{\text{cy}}(k)$ contains the sensitivity of the i-th hedging bond to the j-th cross-yield factor prevailing at time $k\Delta$, and vector $\nabla L_{\text{cy}}(k)$ gathers all liability sensitivities to the same factors. Explicit formulae for all these quantities are derived in Appendix C. These arguments lead to the following:

Portfolio Adjustment Rule: select bond positions meeting the balance condition (18) (resp. (19)) and hedging constraints (21) (resp. (22)).

Clearly, if d is the number of conditions to be met by hedging portfolios, trading must involve no less than $d+1$ bonds. Explicit constraints for the minimal hedging portfolios, *i.e.*, $m = d+1$, are derived in Appendix B, equation (23), and Appendix C, equations (24) and (27). Portfolio selection is performed on all trading dates

$0, \Delta, 2\Delta, ..., (n-1)\Delta = T - \Delta$, leading to a P&L stream for each of the two strategies. In Appendix D, we derive detailed expressions for these quantities.

6.2 Empirical Results

We assess the relative performance of cross-shape risk *vs.* cross-yield risk as a hedging device in the US interest rate market. For the purpose of ascertaining the validity of our findings, we carry out several risk management experiments under alternative parameterizations. However, all trading strategies share a number of common features.

First, within the two examined frameworks, market risk is represented by the first three factors resulting from cross-shape and cross-yield risk analyses over the same time period prior to each trading date. This choice is in agreement with the empirical observation that the first three principal components are the main drivers of bond price variations (Litterman and Scheinkman (1991), Knez *et al.* (1994), Willner (1996), and Lekkos (2001), among others), and further factors are likely to contribute to a negligible extent (Soto (2004)). Cross-shape and cross-yield factor analyses are performed on each trading day over the time series that includes data accrued since the last trade. The resulting cross-shape volatility components $v_1(\tau), ..., v_d(\tau)$ and cross-yield volatility terms $\boldsymbol{v}^1, ..., \boldsymbol{v}^d$ are updated accordingly.

Second, all strategies aim at neutralizing the market risk experienced by a single 8-year liability. This is performed by trading in exactly four coupon bonds, that is, one bond per risk factor plus a position to meet the balance condition. This choice allows us to discard all issues related to asset selection within the (quite larger) basket of tradeable assets in the market. In particular, this contrivance enables us to avoid any bias from the portfolio selection process. The hedging instruments are coupon-bonds with one unit nominal value and maturity equal to 2, 5, 10, and 20 years.

As for the hedging criterion, all first order sensitivities of the liability price to factors are neutralized by selecting a suitable mix of tradeable coupon-bonds. Empirical evidence reported in Kahn and Lochoff (1990), Lacey and Nawalkha (1993), and more recently in Soto (2001), suggests that high-order sensitivities are of minor importance

in representing bond returns when compared to first order terms. Consequently, no constraint is imposed on these quantities and, in particular, on bond price convexities.

All hedging strategies are allowed to adjust at varying frequencies over a one-year trading period and coupons are paid on an annual basis. This allows to avoid considering the technical problem of stripping coupon payments out of the asset values. Also, short sales are allowed for the purpose of forming hedging portfolios. This option has been advocated by several authors such as Chambers, Carleton, and McEnally (1988), Bierwag, Fooladi, and Roberts (1993), and Nawalkha and Chambers (1996), and can be practically achieved through appropriate positions in futures contracts, as noted by Soto (2004).

Finally, all market imperfections such as transaction costs, liquidity constraints and asymmetric creditworthiness of the involved counterparts are ignored.[10]

Risk management strategies differ in terms of 1) factor estimation period, 2) trading period, and 3) hedging frequency.

The factor estimation period is defined as the interval prior to each portfolio adjustment date determining the time series of yield curves on which factors are estimated. By varying this parameter, we can measure the relative importance of old *vs.* recent market volatility in explaining the current structure of market risk. We consider both fixed and floating periods. In the former case, factors are computed from data spanning a fixed number of days by progressively replacing data in the farthest end of the period with recent observations. In the latter case, all new information accrues over the existing one. Following a suggestion by Soto (2004), on each trading day we compute the standing risk factors by using all data available on the same day.

The trading period is the calendar year over which active risk management is carried out. This parameter allows us to check for time consistency and statistical robustness in our findings. We consider several consecutive one-year periods starting on March 1, 1993.

The hedging frequency is the pace at which a hedging portfolio is adjusted to reflect updated market conditions. Following the back-testing scheme in Barone-Adesi, Giannopoulos, and Vosper (2002), we consider 1-day, 2-day, 5-day, and 10-day

adjustment frequencies. This parameter allows us to investigate the convergence speed of a strategy performance to the ideal situation represented by a perfect hedge.

Once a value for each of these three parameters is selected, the risk management test described in the previous section is performed and a pair of P&L streams are recorded, the former corresponding to the cross-shape strategy, the latter stemming from the cross-yield strategy. The empirical distributions of the two P&L streams represent an important device for assessing the quality of the corresponding risk measures. If hedging is perfect, then distributions shrink to zero. Descriptive statistics (*e.g.*, mean, standard deviation, skewness, and kurtosis excess) constitute our main tool to assess the proximity of a P&L stream to the ideal situation of a perfect hedge. In reality, P&L streams substantially deviate from this benchmark. There are three main reasons for this effect. First, yield curve movements need not be linear in the underlying factors, whereas the selected strategy hedges against a first order approximation of yield curve deformations. Next, a perfect hedge would require trading in continuous time, while our hedging portfolio is adjusted on a periodic basis.[11] Finally, any model represents an approximation of the actual market behavior. However, these features do not have a significant impact on the *relative* performance of the two strategies.

Our first experiment focuses on the effect of varying factor estimation periods, specifically from one to eight years prior to the first hedging date. Table 2 reports empirical results for risk management strategies performed between March, 1 2000 and February, 28 2001 using weekly trading.[12]

Insert Table 2 about here

In all cases, the P&L returns stay around the benchmark value 0. However, P&L standard deviations corresponding to cross-shape strategies are lower in most cases. In general, we remark a decrease in this figure as the factor estimation period increases until a minimum is reached on the 5-year (resp. 4-year) window in the cross-shape (resp. cross-yield) case. The degree of distributional symmetry is quite stable over the examined parameterization, showing a persistently positive skewness in the cross-shape hedging and a negative skewness in the cross-yield hedging. We detect no

significant trend in the behavior of the P&L kurtosis.

A second experiment examines trading strategies performed over several 1-year periods ranging from 1993-1994 to 2000-2001. Table 3 reports results for risk management strategies featuring daily trading under a two-year factor estimation period.

Insert Table 3 about here

Four out of eight experiments show a noticeably lower standard deviation under cross-shape trading. The remaining cases display a comparable dispersion under both strategies. The two skewness numbers share a common sign in five instances, with highly symmetric shapes exhibited by cross-shape P&L's. We notice a marked difference in tails between the two P&L's: cross-yield strategies deliver P&L distributions with kurtosis excesses from 1.5 to 26 times larger than their cross-shape counterparts.

A third experiment explores the impact of adjusting the portfolio each 1, 2, 5, and 10 days over the hedging performance. Table 4 reports results for risk management strategies carried out in the periods 1995-1996 (Panel A) and 1997-1998 (Panel B) under a two-year factor estimation period.

Insert Table 4 about here

Again the P&L distributions are quite symmetric and centered around the benchmark hedge. Six cases out of eight exhibit a standard deviation with lower values under cross-shape trading, with figures ranging from twenty to fifty percent of the corresponding numbers under cross-yield hedging. Period 1995-1996 (Panel A) has been selected from the worst performing periods for cross-shape trading. Nevertheless, the distributional kurtosis is larger compared to the values obtained under cross-yield trading. Period 1997-1998 (Panel B) represents a typical risk management scenario. In all circumstances, the kurtosis excess increases with the hedging frequency. This phenomenon is explained by the smoothing effect played by infrequent portfolio rebalancing compared to trading with frequent response to local market perturbations. Kurtosis from cross-shape trading is always smaller (and more slowly increasing over time) than the corresponding figure under cross-yield hedging. Figure 5 displays empirical P&L distributions estimated by a Gaussian kernel for experiments conducted

over the periods 1994-1995 (left-hand graph) and 1997-1998 (right-hand graph) .

Insert Figure 5 about here

These curves highlight an important property of cross-shape risk. Specifically, the P&L distribution from cross-shape hedging is much closer to the Gaussian density sharing the same mean and variance than the P&L distribution from cross-yield hedging. In particular, the former displays thinner tails than the latter. Moreover, this feature implies that the standard tools of Gaussian approximations adopted for Value-at-Risk measures of fixed-income portfolios deliver more accurate risk assessments in a framework based on cross-shapes than they can do in a cross-yield setting.

It is worth noticing that all the above experiments have been conducted using yield data with evenly staggered tenors and basis functions spanning the yield curve range quite uniformly. Our final experiment relaxes these assumptions and investigates the impact of the selected functional basis on the quality of risk management. We repeated the second experiment stated above using alternative classes of interpolating functions, namely exponentially weighed Laguerre and Chebyshev polynomials.

Insert Table 5 about here

The results reported in Table 5 exhibit a strong bias and instability across time in the descriptive statistics of P&L distributions from cross-shape strategies grounded on Chebyshev basis functions compared to those resulting from Laguerre shapes. A similar conclusion can be obtained by comparing the performance of cross-yield strategies computed on terms structures with tenors displaying varying levels of uniformity, a fact that has been rarely pointed out in the existing literature. Consequently, the final user should put a particular care in 1) selecting observed yields on uniformly spanned times-to-maturity and 2) identifying a class of basis functions covering the range of admissible yield curves as uniformly as possible.

In summary, the notion of cross-shape risk introduced in this paper remarkably improves the sample performance of traditional immunization strategies.

7 Conclusion

Yield curve changes represent the main determinant of interest rate market risk. Consequently, the risk management of investment portfolios requires a careful assessment of factors driving yield curve dynamics. The existing literature is divided between the analytic description of possible yield curve deformations and the quantitative measurement of risk borne by limited portions of the curve.

Our proposal fills in the gap between the two methodologies. We introduced a new measure of cross-sectional risk linking yield curve shapes and market volatility. This measure, which is rooted in the empirical investigations carried out by Litterman, Scheinkman, and Weiss (1991) and Engle and Ng (1993), goes beyond the traditional cross-yield covariance introduced by Steeley (1990) and Litterman and Scheinkman (1991). We developed our theory for general cross-sectional data, detailed an econometric procedure to decompose cross-shape risk into analytic cross-sectional deformations, and provides an expression for all cross-yield covariances in terms of our cross-shape risk factors.

On the empirical side, we focused on the US Treasury Bond market and compared cross-shape and cross-yield risk measures according to their performance as a market risk measure and as a risk management tool. An empirical test showed that a limited number of cross-shape factors accounts for interest rate risk better than the same number of cross-yield factors. A further experiment exhibited that the vast majority of trading simulations immunizing against cross-shape risk deliver less volatile P&L distributions than those resulting from strategies hedging against cross-yield risk.

Our methodology can be applied to any market delivering time series of quoted cross-sections. Further applications may include risk analysis and management in equity, commodity, and option markets.

Footnotes

1. Fong and Vasiček (1984) and Balbás and Ibáñez (1998), among others, propose non-factorial methods to immunize bond portfolios against yield shifts. We do not consider this literature since our main concern here is factor modeling of yield curve dynamics.

2. Relevant dimensions include time-to-maturity for bond prices, equity size and book-to-market for equity prices, moneyness and time-to-expiration for option prices.

3. Key rates and cross-yield principal components provide no assessment about the risk experienced by the unobservable portions of the yield curve.

4. Factors z_j and errors ε_i are supposed to satisfy appropriate distributional assumptions (see Knez, *et al.* (1995)). In particular, yield returns over different time periods share a common distribution, so that the corresponding process is time-homogeneous.

5. One-unit standard deviation in the j-th noise component z_j generates $v_j(\tau)$ units of standard deviation in the yield increment corresponding to a time-to-maturity τ.

6. Ho (1992) and Golub and Tilman (1997) describe trading strategies based on key rates.

7. Usually the 2, 5, and 10-year yields are stripped from T-bonds, while other yields, *e.g.*, the 6-month, 1, 7, 15, and 20-year yields, are obtained from other liquid instruments. No transaction cost is included.

8. Other popular classes suffer from severe drawbacks. Piecewise linear yield curves introduce discontinuities in forward rates, generating instability in the value of interest rate derivatives. Purely polynomial curves produce implausible oscillations between interpolated yields, stimulating traders to enter positions in the less liquid, and riskier, portions of the curve. Empirical experiments suggest that the smoothing parameter ζ should be selected between 0.3 and 0.5. Our results turn out to be quite similar across all values of ζ in this range.

9. Geman, El Karoui, and Lacoste (2000) detail the method within arbitrage-free dynamics.

10. Transaction costs may be relevant for an empirical investigation of the absolute performance of our methodology, a topic which is not dealt with in the present study. Here, we focus instead on the relative performance of our method in comparison with the up-to-date

best performing alternative (standard PCA). Notice however that trading involves highly liquid on-the-run bonds, for which the bid-ask spread is typically a fraction of a basis point. Consequently, including transaction costs has a negligible effect on the absolute performance of the method over the time horizon we considered.

11. We suppose the underlying market is complete. This condition is met by assuming that as many bonds can be traded as the number of the underlying independent factors.

12. One working week consists of five consecutive sample dates in the data set.

Acknowledgements

We would like to thank Claudio Albanese, Marco Avellaneda, Giovanni Barone Adesi, Francesco Corielli, Rita Laura D'Ecclesia, José Miguel Gaspar, Hélyette Geman, Eugenia Shlimovich, the seminar participants at Bocconi University, Imperial College, Tilburg University, the 32nd European Finance Association Meeting (Moscow, August 2005), the IFORS Congress (Honolulu, July 2005), the International Summer School on Risk Management and Control (Rome, June 2005), the Third International Bachelier Congress (Chicago, July 2004), the Quantitative Methods in Finance Conference (Cairns and Sydney, December 2002), the Editor, and the two anonymous referees for valuable comments. The usual disclaimers apply. Roncoroni gratefully acknowledges financial support from CERESSEC. We wish to thank BNP Paribas for kindly providing data.

References

[1] Anderson, N., Breedon F., Deacon M., Derry A., Murphy G., 1996, Estimating and Interpreting the Yield Curve, John Wiley & Sons, New York.

[2] Balbás, A., Ibáñez, A., 1998. When can you immunize a bond portfolio? Journal of Banking and Finance 22, 1571-1595.

[3] Barber, J.R., Copper, M.L., 1996. Immunization using principal components analysis. Journal of Portfolio Management (Summer), 99-105.

[4] Barone-Adesi, G., Giannopoulos, K., Vosper, L., 2002. Backtesting derivative portfolios with filtered historical simulation (FHS), European Financial Management 8 (1), 31-58.

[5] Barrett, W.B., Gosnell T.F., Heuson, A.J., 1995. Yield Curve Shifts and the Selection of Immunization Strategies. Journal of Fixed Income (Sept.), 53-64.

[6] Bierwag, G.O., Fooladi, I., Roberts, G.S., 1993. Designing an immunized portfolio: Is M-squared the key? Journal of Banking and Finance 17, 1147-1170.

[7] Chambers, D.R., Carleton, W.T., McEnally, R.W., 1988. Immunizing default-free bond portfolios with a duration vector. Journal of Financial and Quantitative Analysis 23, 89-104.

[8] Cox, J.C., Ingersoll, J.E., Ross, S.A., 1985. A theory of the term structure of interest rates. Econometrica 53, 385-408.

[9] Elton, E.J., Gruber, M.J., Michaely, R., 1990. The structure of spot rates and immunization. Journal of Finance 45, 629-642.

[10] Engle, R.F., Ng, V.K., 1993. Time-varying volatility and the dynamic behavior of the term structure. Journal of Money, Credit and Banking 25(3), 336-349.

[11] Fama, E.F., French, K.R., 1992. The Cross-Section of Expected Stock Returns. Journal of Finance 47, 427-465.

[12] Fisher, L., Weil, R.L., 1971. Coping with the risk of interest rate fluctuations: Returns to bondholders from naive and optimal strategies. Journal of Business 44, 408-431.

[13] Fong, H.G., Vasiček, O.A., 1984. A risk minimizing strategy for portfolio immunization. Journal of Finance 39, 1541-1546.

[14] Geman, H., El Karoui, N., Lacoste, V., 2000. On the Role of State Variables in Interest Rates Models. Applied Stochastic Models in Business and Industry 16, 197-217.

[15] Golub, B.W., Tilman, L.M., 1997. Measuring yield curve risk using principal components analysis, value at risk, and key rate durations. Journal of Portfolio Managemant (Summer), 72-84.

[16] Heath, D., Jarrow, R., Morton, A., 1992. Bond pricing and the term structure of interest rates: A new methodology. Econometrica 61, 77-105.

[17] Ho, T.S.Y., 1992. Key rate durations: Measures of interest rate risk. Journal of Fixed Income (September), 29-44.

[18] Hull, J., 2005. Options, Futures, and Other Derivatives (6th ed.). Prentice Hall, New Jersey.

[19] Kahn, R.N., Lochoff, R., 1990. Convexity and exceptional return. Journal of Portfolio Management (Winter), 43-47.

[20] Knez, P.J., Litterman, R., Scheinkman, J., 1994. Explorations into factors explaining money market returns. Journal of Finance 5, 1861-1882.

[21] Lacey, N.J., Nawalkha, S.K., 1993. Convexity, risk and returns. Journal of Fixed Income (December), 72-79.

[22] Lekkos, I., 2001. Factor models and the correlation structure of interest rates: Some evidence for USD, GBP, DEM and JPY. Journal of Banking and Finance 25, 1427-1445.

[23] Litterman, R., Scheinkman, J., 1991. Common factors affecting bond returns. Journal of Fixed Income 1 (June), 54-61.

[24] Litterman, R., Scheinkman, J., Weiss, L., 1991. Volatility and the Yield Curve. Journal of Fixed Income 1 (June), 49-53.

[25] Nawalkha, S.K., Chambers, D.R., 1996, An improved immunization strategy: M-absolute. Financial Analysts Journal (September/October), 69-76.

[26] Pérignon, C., Villa, C., 2006 (*to appear*). Sources of time variation in the covariance matrix of interest rates. Journal of Business 79(6).

[27] Phoa, W., Shearer, M., 1997. A note on arbitrary yield curve reshaping sensitivities using key rate durations. Journal of Fixed Income (December), 67-71.

[28] Prisman, E.Z., Shores, M.R., 1988. Duration measures for specific term structure estimations and applications to bond portfolio immunization. Journal of Banking and Finance 12, 493-504.

[29] Redington, F.M., 1952. Review of the principles of life-office valuations. Journal of the Institute of Actuaries 18, 286-340.

[30] RiskMetrics, 1996. Riskmetrics: Technical Document, fourth ed.

[31] Rodrigues de Almeida, C.I., Duarte Jr., A.M, Coelho Fernandes, C.A., 1998. Decomposing and simulating the movements of term structures of interest rates in emerging Eurobond markets. Journal of Fixed Income (June), 21-31.

[32] Soto, G.M., 2001. Immunization derived from a polynomial duration vector in the Spanish bond market. Journal of Banking and Finance 25, 1037-1057.

[33] Soto, G.M., 2004. Duration models and IRR management: A question of dimensions? Journal of Banking and Finance 28 (5), 1089-1110.

[34] Steeley, J.M., 1990. Modelling the dynamics of the term structure of interest rates. Economic and Social Review 21, 337-361.

[35] Willner, R., 1996. A new tool for portfolio managers: Level, slope and curvature durations. Journal of Fixed Income (June), 48-59.

A Appendix: Alternative Bases

We consider three bases. Each basis is a set of functions

$$\psi_l(\tau) := \mathcal{L}_l(\tau) \exp(-\zeta\tau), \qquad l = 1, ..., N.$$

Here ζ is a positive constant and $\mathcal{L}_l(\tau)$ denotes the l-th polynomial in either of the following three classes (each polynomial being defined as a solution of an equation that we report together with its first three solutions):

1) Laguerre polynomials.

Definition: $\tau\mathcal{L}_l''(\tau) + (1-\tau)\mathcal{L}_l'(\tau) + l\mathcal{L}_l(\tau) = 0.$
Solutions: $\mathcal{L}_0(\tau) = 1, \mathcal{L}_1(\tau) = 1-\tau, \mathcal{L}_2(\tau) = \frac{1}{2}\left(2 - 4\tau + \tau^2\right).$

2) Legendre polynomials.

Definition: $\left(1-\tau^2\right)\mathcal{L}_l''(\tau) - 2\tau\mathcal{L}_l'(\tau) + l(l+1) = 0.$
Solutions: $\mathcal{L}_0(\tau) = 1, \mathcal{L}_1(\tau) = \tau, \mathcal{L}_2(\tau) = -\frac{1}{2} + \frac{3\tau^2}{2}.$

3) Chebyshev polynomials.

Definition: $\mathcal{L}_l(\tau) = \cos(l \arccos(\tau)).$
Solutions: $\mathcal{L}_0(\tau) = 1, \mathcal{L}_1(\tau) = \tau, \mathcal{L}_2(\tau) = -1 + 2\tau^2.$

B Appendix: Balance Conditions

The cheapest portfolio that hedges against a number d of independent factors needs to contain $m = d+1$ securities. In this case, *par* conditions $B_\alpha(0) = N^\alpha$, $\alpha = 0, ..., d+1$, lead to explicit expressions for the initial balance constraints (20):

$$\sum_{\alpha=1}^{d+1} N^\alpha q_\alpha(0) = N^0, \qquad \sum_{\alpha=1}^{d+1} N^\alpha \chi_\alpha(0) = N^0,$$

where $q_\alpha(0)$ (resp. $\chi_\alpha(0)$) denotes the initial quantity of bond α in the portfolio selection under a cross-shape (resp. cross-yield) strategy. The running balance conditions state that the current value of the rebalanced portfolio must match the current value

of the standing portfolio plus any increase in the market value of the outstanding liability, that is

$$\sum_{\alpha=1}^{d+1}\sum_{i=1}^{n^\alpha} c^\alpha p_{k,i} q_\alpha(k) = \sum_{\alpha=1}^{d+1}\sum_{i=1}^{n^\alpha} c^\alpha p_{k,i} q_\alpha(k-1) + \sum_{i=1}^{n^0} c^0 \left[p_{k,i} - p_{k-1,i}\right], \tag{23}$$

where $p_{k,i}$ denotes the discount factor prevailing on the current date $k\Delta$ for the i-th coupon payment time $i - k\Delta$. We notice that $p_{k,i}$ is defined for all $i = 1, ..., \max_\alpha n^\alpha$, namely the last coupon payment date in the basket of tradeable bonds. Self-financing conditions for the cross-yield strategy can be derived by simply replacing q with χ in the above expression.

C Appendix: Hedging Constraints

We begin by deriving the first-order constraints for the cross-shape strategy and then move to calculate the corresponding conditions for the cross-yield strategy.

Let $\tau_{k,i} = i - (k-1)\Delta$ denote the period (in years) between the k-th trading day ($k = 1, ..., n$) and the payment date of the i-th coupon. The discount bond sensitivity to the j-th cross-shape factor is given by $\partial_j P(t,\tau) = -\tau P(t,\tau) v_j(\tau)$. Since day k price of the α-th hedging bond is $\sum_{i=1}^{n^\alpha} c^\alpha p_{k,i}$, then the corresponding sensitivity to the j-th factor reads as $-\sum_{i=1}^{n^\alpha} c^\alpha \tau_{k,i} v_j(\tau_{k,i}) p_{k,i}$. The same formula holds for the outstanding liability, with $\alpha = 0$. A bond portfolio sensitivity to the same factor can be expressed as $-\sum_{\alpha=1}^{n^{d+1}}\sum_{i=1}^{n^\alpha} c^\alpha \tau_{k,i} v_j(\tau_{k,i}) p_{k,i}$. Consequently, the hedging portfolio is required to satisfy the following set of conditions:

$$\nabla \mathbf{B}_{\text{cs}}(k) \cdot \mathbf{q}(k) = \nabla L_{\text{cs}}(k), \tag{24}$$

where $\mathbf{q}$ is the $(d+1)$-dimensional vector of bond positions,

$$\nabla \mathbf{B}_{\text{cs}}(k) = \begin{pmatrix} \sum_{i=1}^{n^1} c^1 \tau_{k,i} v_1(\tau_{k,i}) p_{k,i} & \dots & \sum_{i=1}^{n^{d+1}} c^{d+1} \tau_{k,i} v_1(\tau_{k,i}) p_{k,i} \\ \sum_{i=1}^{n^1} c^1 \tau_{k,i} v_2(\tau_{k,i}) p_{k,i} & \dots & \dots \\ \dots & & \\ \sum_{i=1}^{n^1} c^1 \tau_{k,i} v_d(\tau_{k,i}) p_{k,i} & & \sum_{i=1}^{n^{d+1}} c^{d+1} \tau_{k,i} v_d(\tau_{k,i}) p_{k,i} \end{pmatrix} \tag{25}$$

is a $d \times (d+1)$ matrix gathering raw-wise all coupon-bond sensitivities to the d cross-shape factors and

$$\nabla L_{\text{cs}}(k) = \begin{pmatrix} \sum_{i=1}^{n^0} c^0 \tau_{k,i} v_1(\tau_{k,i}) p_{k,i} \\ \sum_{i=1}^{n^0} c^0 \tau_{k,i} v_2(\tau_{k,i}) p_{k,i} \\ \dots \\ \sum_{i=1}^{n^0} c^0 \tau_{k,i} v_d(\tau_{k,i}) p_{k,i} \end{pmatrix} \tag{26}$$

is a d-dimensional vector containing all liability sensitivities to the d cross-shape factors.

If risk is measured by a cross-yield covariance, the hedging conditions read as

$$\nabla \mathbf{B}_{\text{cy}}(k) \cdot \boldsymbol{\chi}(k) = \nabla L_{\text{cy}}(k), \tag{27}$$

where $\boldsymbol{\chi}$ is the $(d+1)$-dimensional vector of bond positions and sensitivities $\nabla \mathbf{B}_{\text{cy}}$ and ∇L_{cy} are computed according to the chosen interpolation method. Specifically, these quantities obtain by replacing functions v_j in formulae (25) and (26) with interpolating sensitivity functions

$$v_j^*(\tau) = \partial_k y(\tau) v_k^j, \quad j = 1, ..., d.$$

Here $y(\tau) = \sum_{l=1}^{N} b_l(y(\tau_1), ..., y(\tau_N)) \psi_l(\tau)$ is the yield curve interpolating yields $y(\tau_1), ..., y(\tau_N)$, $\partial_k y(\tau) = \frac{\partial y(\tau)}{\partial y(\tau_k)}$ measures the sensitivity of a recovered yield $y(\tau)$ to a small shock in the observed yield $y(\tau_k)$, and v_k^j is the k-th entry of the eigenvector corresponding to the j-th greatest eigenvalue of the empirical cross-yield covariance matrix.

D Appendix: Profit and Loss Streams

Let $\mathrm{P\&L_{cs}} = (\mathrm{P\&L_{cs}}(1), ..., \mathrm{P\&L_{cs}}(n))$ (resp. $\mathrm{P\&L_{cy}} = (\mathrm{P\&L_{cy}}(1), ..., \mathrm{P\&L_{cy}}(n))$) denote the sequence of profits and losses resulting from the cross-shape (resp. cross-yield) strategy on the trading dates $\Delta, 2\Delta, ..., (n-1)\Delta$ and the final day $n\Delta$. According to expressions (16) and (17) in section 6, a single P&L occurring on day k is given by the difference in value between the hedging portfolio and the outstanding liability. The former involves $d+1$ positions in coupon-bonds, each position being determined one time step before as $q_\alpha(k-1)$. The latter is just the present value of the outstanding liability.

$$\begin{aligned}
\mathrm{P\&L_{cs}}(k) &= \sum_{\alpha=1}^{d+1}\sum_{i=1}^{n^\alpha} c^\alpha p_{k,i} q_\alpha(k-1) - \sum_{i=1}^{n^0} c^0 p_{k,i}, \\
\mathrm{P\&L_{cy}}(k) &= \sum_{\alpha=1}^{d+1}\sum_{i=1}^{n^\alpha} c^\alpha p_{k,i} \chi_\alpha(k-1) - \sum_{i=1}^{n^0} c^0 p_{k,i}.
\end{aligned}$$

Table 1
Cumulative percentage variance borne by the one, two, three, and four most significant cross-shape and cross-yield factors.

Time Period	**March, 1st 88-91**		**March, 1st 91-94**		**March, 1st 94-97**		**March, 1st 97-02**	
Factor Type	**Standard**	**Shape**	**Standard**	**Shape**	**Standard**	**Shape**	**Standard**	**Shape**
Factor 1	78,09	78,76	76,48	77,19	91,03	82,47	86,07	81,29
Factors 1+2	92,58	97,11	90,65	95,37	97,74	97,29	97,22	97,36
Factors 1+2+3	96,35	99,14	94,64	99,02	98,95	99,56	98,83	99,52
Factors 1+2+3+4	98,05	99,83	96,58	99,68	99,50	99,95	99,44	99,96

Each entry displays the percentage of historical variance explained by the corresponding number of factors as defined according to the indicated type of risk analysis.

Table 2
Descriptive Statistics of Hedging P&L's under Varying Factor Identification Periods.

Panel A: 1-year to 4-year Identification Periods.

	1 year		2 years		3 years		4 years	
Factor Type	**Standard**	**Shape**	**Standard**	**Shape**	**Standard**	**Shape**	**Standard**	**Shape**
Average (x 0.1%)	0.00	0.00	-0.01	-0.01	-0.03	-0.01	-0.03	-0.03
Std. Dev. (x 0.1%)	0.92	0.87	1.00	0.90	0.87	0.84	0.79	0.83
Skewness	-0.31	0.44	-0.45	0.48	-0.46	0.50	-0.38	0.50
Kurtosis Excess	0.05	-0.34	0.24	0.09	0.22	-0.03	0.18	-0.21

Panel B: 5-year to 8-year Identification Periods.

	5 years		6 years		7 years		8 years	
Factor Type	**Standard**	**Shape**	**Standard**	**Shape**	**Standard**	**Shape**	**Standard**	**Shape**
Average (x 0.1%)	-0.03	-0.03	-0.03	-0.05	-0.01	-0.01	-0.07	-0.11
Std. Dev. (x 0.1%)	0.85	0.73	0.69	0.77	0.94	0.99	0.92	1.30
Skewness	-0.18	0.42	-0.06	0.43	-0.69	-0.56	0.18	0.54
Kurtosis Excess	0.07	-0.32	-0.05	-0.40	0.31	-0.11	0.11	-0.12

Descriptive statistics of hedging P&L's distributions are computed for trading strategies based on standard yield risk and shape risk estimated on different time periods prior to each portfolio adjustement date. Estimation is performed on floating time windows ranging from 1 to 8 years. Strategies span the period between March, 1 2000 and February, 28 2001, and corresponding portfolios are adjusted every 5 business days.

Table 3
Descriptive Statistics of Hedging P&L's under Varying 1-Year Trading Periods.

Panel A: 1-year Trading Periods from 1993 to 1996.

	1993 - 1994		1994 - 1995		1995 - 1996		1996 - 1997	
Factor Type	**Standard**	**Shape**	**Standard**	**Shape**	**Standard**	**Shape**	**Standard**	**Shape**
Average (x 0.1%)	-0.54	-0.17	0.05	0.00	0.01	0.01	-0.01	0.01
Std. Dev. (x 0.1%)	9.32	2.34	0.51	0.38	0.31	0.30	0.38	0.29
Skewness	-2.48	-3.41	1.25	0.20	0.54	-0.11	0.59	0.46
Kurtosis Excess	59.78	31.51	6.27	0.24	5.68	1.19	3.93	2.61

Panel B: 1-year Trading Periods from 1997 to 2000.

	1997 - 1998		1998 - 1999		1999 - 2000		2000 - 2001	
Factor Type	**Standard**	**Shape**	**Standard**	**Shape**	**Standard**	**Shape**	**Standard**	**Shape**
Average (x 0.1%)	0.00	0.00	0.00	0.00	0.00	0.00	-0.01	0.01
Std. Dev. (x 0.1%)	0.44	0.33	0.37	0.38	0.32	0.45	0.32	0.36
Skewness	-0.93	0.21	0.41	-0.65	-1.12	-0.11	0.36	0.07
Kurtosis Excess	11.72	0.97	3.97	0.23	2.51	0.36	1.55	-0.08

Descriptive statistics of hedging P&L's distributions are computed for trading strategies based on standard yield risk and shape risk estimated on a 2-year time window prior to the first trading day and then updated at each portfolio adjustment. Trading is performed on 8 consecutive 1-year periods, starting on March, 1 1993 and ending on February, 28 2001. Corresponding portfolios are adjusted every business day.

Table 4
Descriptive Statistics of Hedging P&L's under Varying Portfolio Adjustment Frequency.

Panel A: Trading from March, 1st 1995 to February, 28 1996.

	10 days		5 days		2 days		1 day	
Factor Type	**Standard**	**Shape**	**Standard**	**Shape**	**Standard**	**Shape**	**Standard**	**Shape**
Average (x 0.1%)	0.12	-0.17	0.06	-0.19	0.02	-0.07	0.01	0.00
Std. Dev. (x 0.1%)	0.71	0.37	0.65	0.34	0.38	0.45	0.31	0.30
Skewness	-0.48	-0.52	-0.03	-0.32	0.54	-0.93	0.54	-0.11
Kurtosis Excess	1.02	1.50	0.42	1.18	2.87	3.14	5.68	1.19

Panel B: Trading from March, 1st 1997 to February, 28 1998.

	10 days		5 days		2 days		1 day	
Factor Type	**Standard**	**Shape**	**Standard**	**Shape**	**Standard**	**Shape**	**Standard**	**Shape**
Average (x 0.1%)	-0.01	-0.01	0.00	0.00	0.00	0.00	0.00	0.00
Std. Dev. (x 0.1%)	1.17	0.72	0.85	0.50	0.55	0.45	0.44	0.33
Skewness	-0.62	0.43	-0.89	-0.76	-1.30	-0.10	-0.93	0.21
Kurtosis Excess	0.31	-0.27	2.66	0.64	6.83	0.30	11.72	0.97

Descriptive statistics of hedging P&L's distributions are computed for trading strategies based on standard yield risk and shape risk estimated on a 2-year time window prior to the first trading day and then updated at each portfolio adjustment. Trading is performed on two 1-year periods: March, 1 1995 - February, 28 1996 (Panel A), March, 1 1997 - February, 28 1998 (Panel B). Corresponding portfolios are adjusted at frequencies of 1, 2, 5, and 10 days.

Table 5
Descriptive Statistics of Hedging P&L's under Varying 1-Year Trading Periods and Alternative Shape Risk Assessments.

Panel A: 1-year Trading Periods from 1993 to 1996.

	1993 - 1994		1994 - 1995		1995 - 1996		1996 - 1997	
Factor Type	**Chebyshev**	**Laguerre**	**Chebyshev**	**Laguerre**	**Chebyshev**	**Laguerre**	**Chebyshev**	**Laguerre**
Average (x 0.1%)	-0,20	-0,17	-0,80	0,00	-0,30	0,01	-0,10	0,01
Std. Dev. (x 0.1%)	3,00	2,34	53,20	0,38	46,00	0,30	7,65	0,29
Skewness	-2,66	-3,41	-12,42	0,20	-1,34	-0,11	0,24	0,46
Kurtosis Excess	32,10	31,51	188,64	0,24	106,38	1,19	21,00	2,61

Panel B: 1-year Trading Periods from 1997 to 2000.

	1997 - 1998		1998 - 1999		1999 - 2000		2000 - 2001	
Factor Type	**Chebyshev**	**Laguerre**	**Chebyshev**	**Laguerre**	**Chebyshev**	**Laguerre**	**Chebyshev**	**Laguerre**
Average (x 0.1%)	0,00	0,00	-28,00	0,00	0,00	0,00	0,90	0,01
Std. Dev. (x 0.1%)	0,38	0,33	327,00	0,38	2,10	0,45	14,00	0,36
Skewness	0,22	0,21	-5,60	-0,65	0,22	-0,11	4,70	0,07
Kurtosis Excess	1,06	0,97	61,00	0,23	1,92	0,36	38,00	-0,08

Descriptive statistics of hedging P&L's distributions are computed for trading strategies based on shape risk estimated on a 2-year time window prior to the first trading day and then updated at each portfolio adjustment. Shape risk is alternatively evaluated by using smoothed Chebyshev and Laguerre polynomials. Trading is performed on 8 consecutive 1-year periods, starting on March, 1 1993 and ending on February, 28 2001. Corresponding portfolios are adjusted every business day.

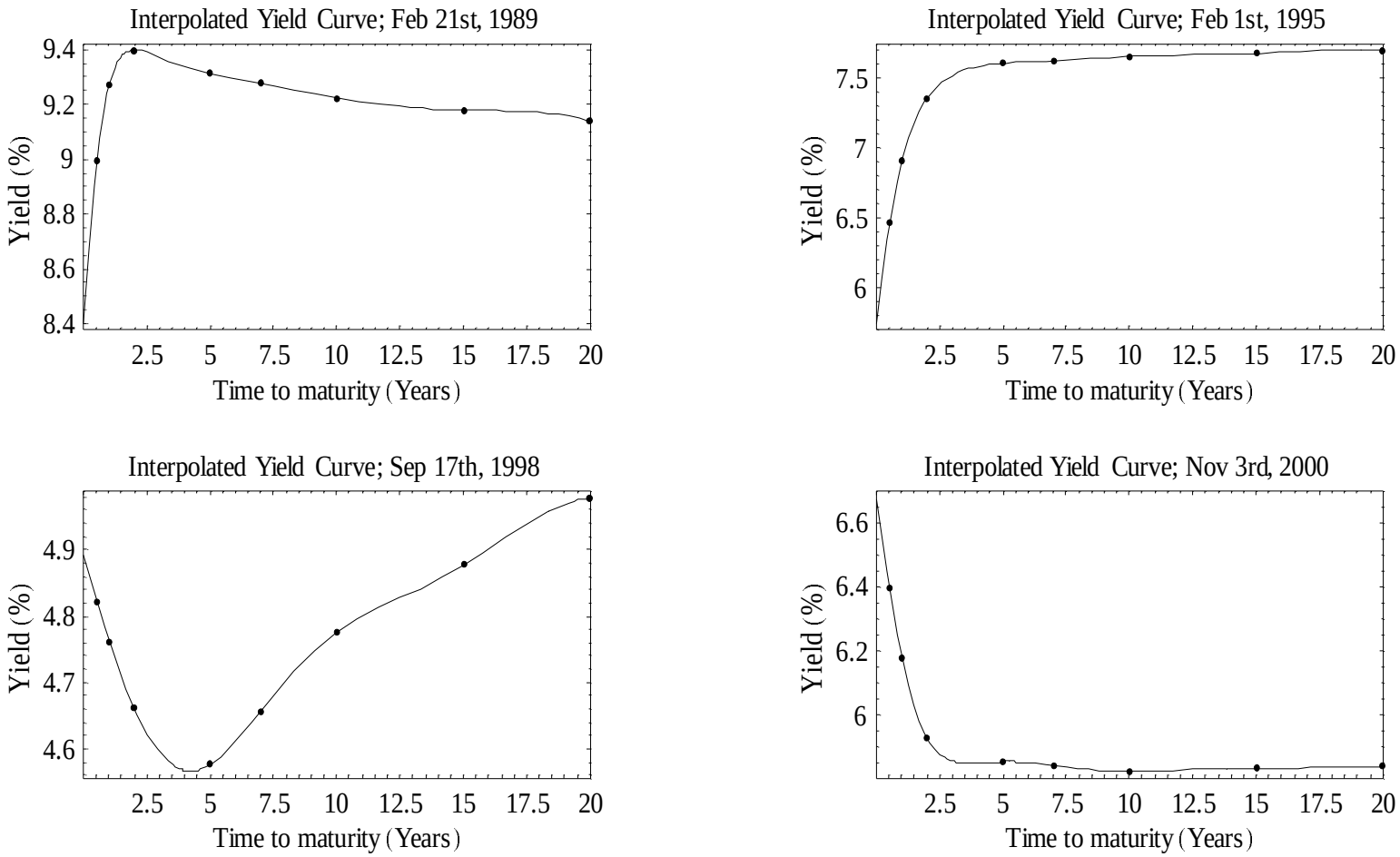

Fig. 1: Qualitatively distinct shapes exibited by sample yield curves: downward humped (upper-left panel), upward humped (lower-left panel), concave (upper-right panel), convex (lower-right panel).

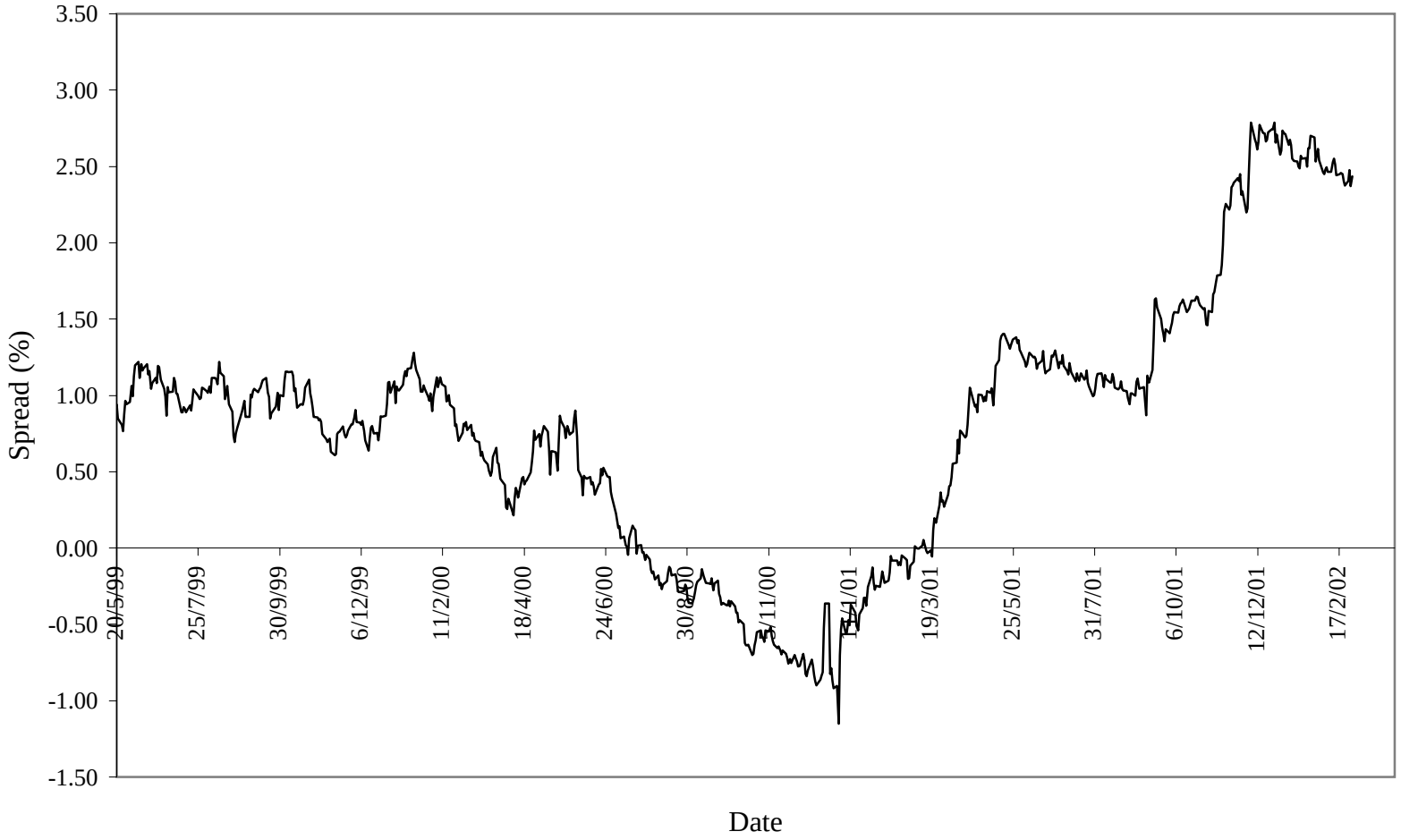

Fig. 2: The 5-year minus 3-month yield spread path in the period from May, 20 1999 to February, 17 2002.

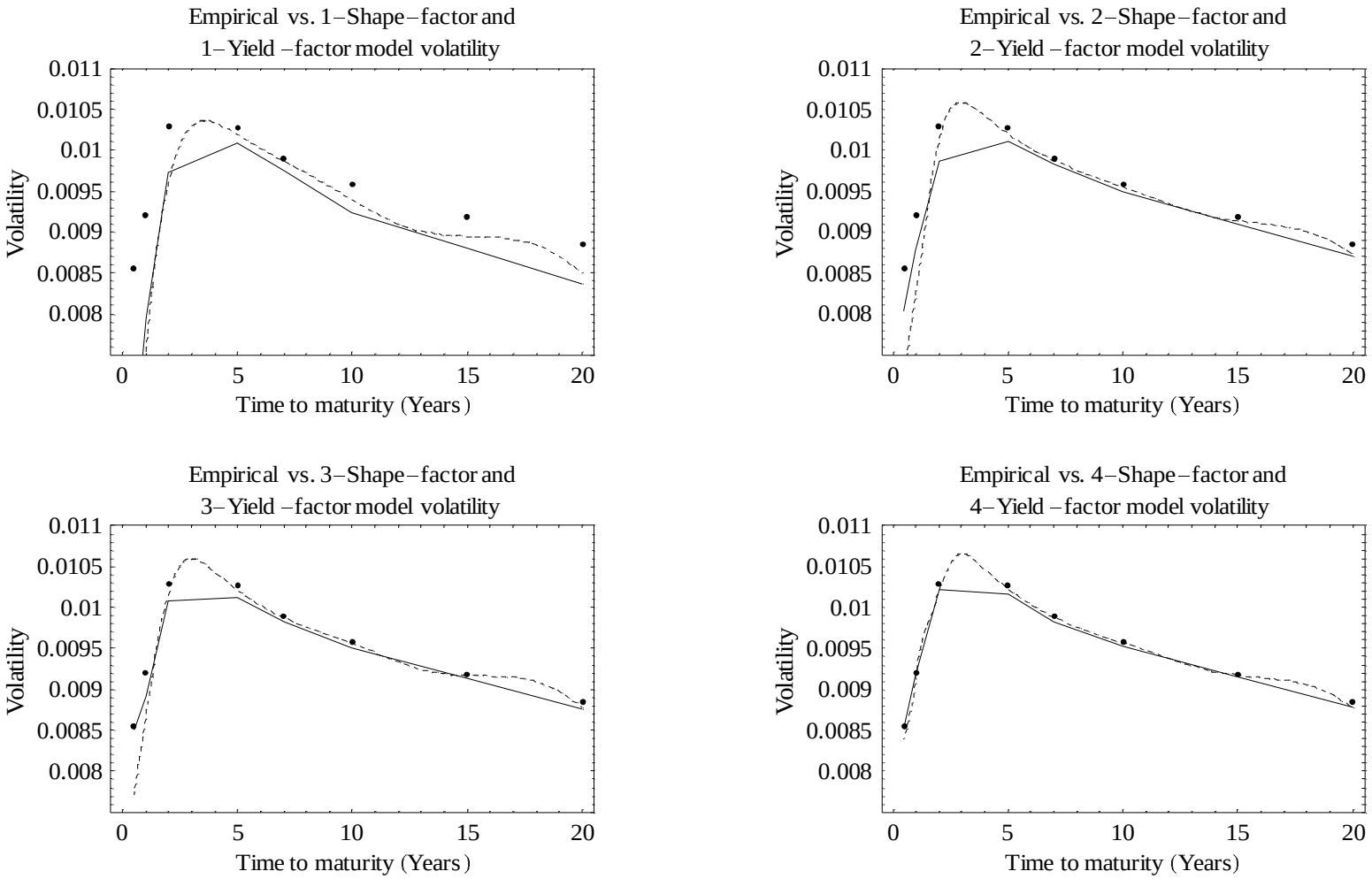

Fig. 3: Historical volatilities at benchmark times to maturity (dots) are compared to volatility curves obtained by the leading 1, 2, 3, and 4 yield factors (plain line) and to volatility curves resulting from the leading 1, 2, 3, and 4 shape factors (dashed curve).

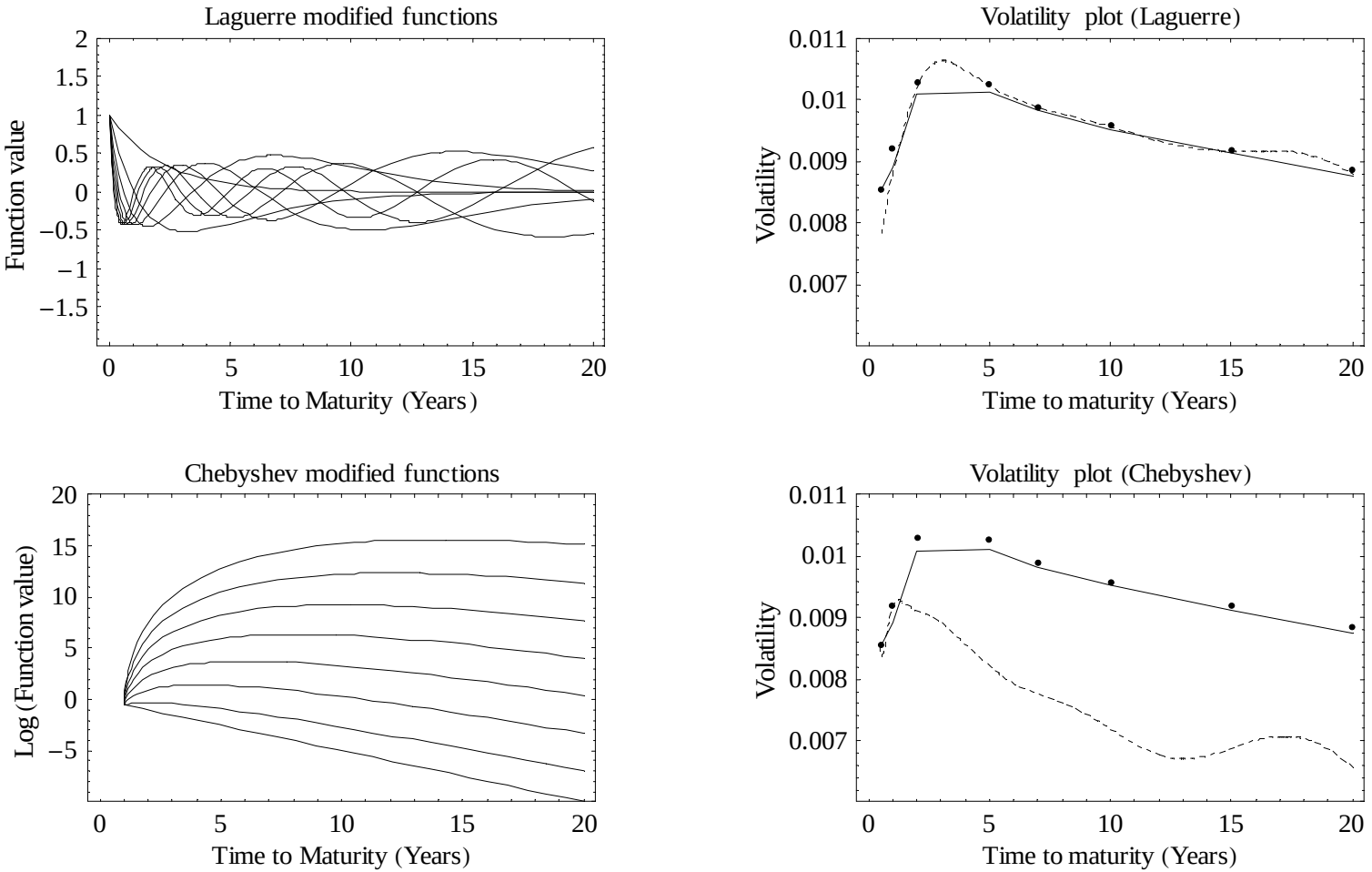

Fig. 4: Historical volatilities at benchmark times to maturity (dots) are compared to volatility curves obtained by the leading 4 shape factors alternatively computed by using smoothed Laguerre (upper graph) and Chebyshev (lower graph) functions. Lefthand graphs show the eight basis functions. It appears evident that the quality of volatility recovery depends on the ability of selected basis functions to uniformly span the range of possibly yield curve variations.

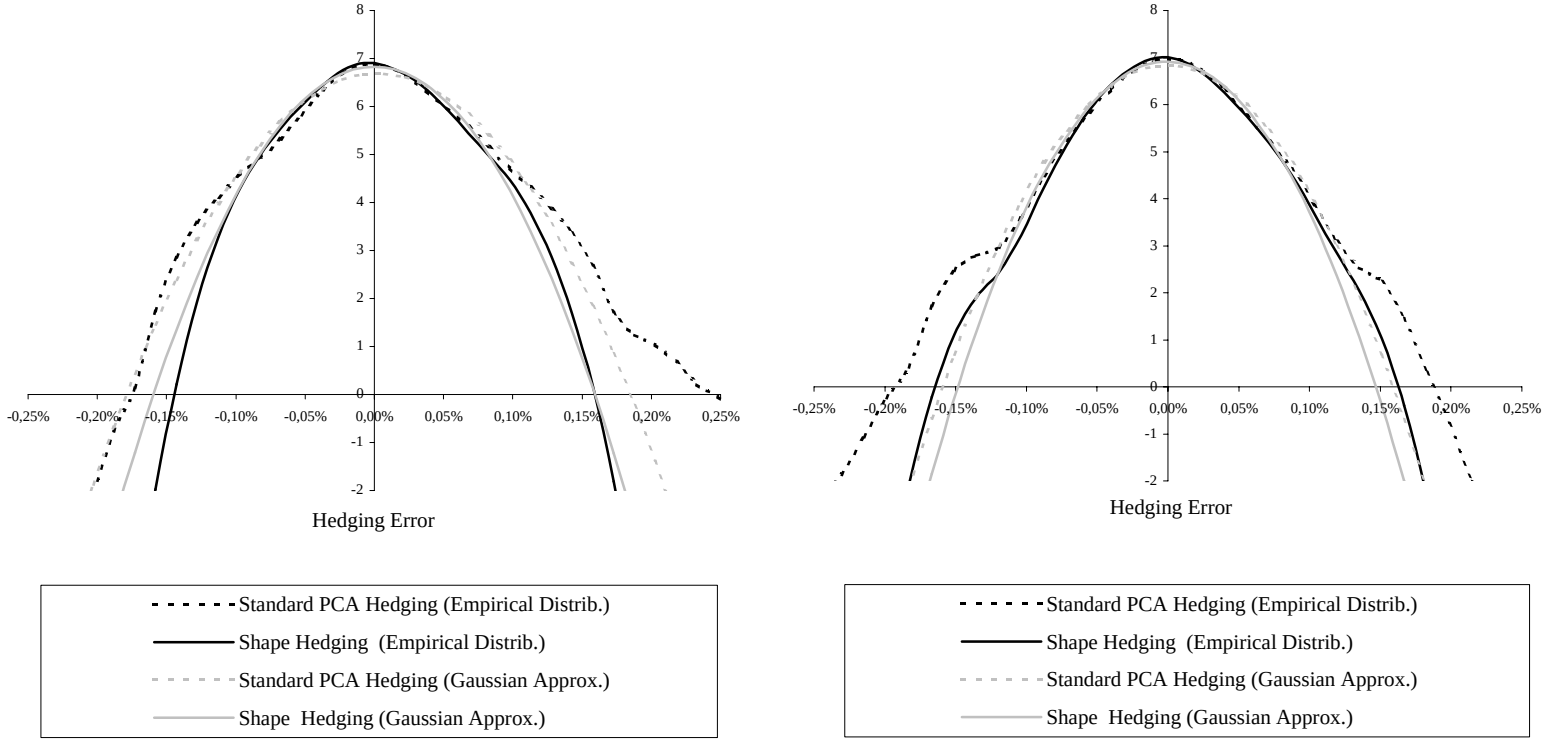

Fig. 5: Empirical probability density functions of logarithmic P&L's stemming from trading in the period 1994-1995 (left) and 1997-1998 (right).